Journal of Earth Science, *Vol. 27*, *No. 5*, *p. 807–822*, *October 2016* *ISSN 1674-487X*
Printed in China
DOI: 10.1007/s12583-015-0592-1

Sedimentary Facies of Marine Shale Gas Formations in Southern China: The Lower Silurian Longmaxi Formation in the Southern Sichuan Basin

Yizhen Li[1, 2], **Xingzhi Wang***[1], **Bin Wu**[3], **Guoqin Li**[1, 2], **Dule Wang**[1]
1. *State Key Laboratory of Oil and Gas Reservoir Geology and Exploitation*, *Southwest Petroleum University*, *Chengdu* 610500, *China*
2. *Geological Exploration and Development Research Institute*, *CNPC Chuanqing Drilling Engineering Company Limited*, *Chengdu* 610051, *China*
3. *Chongqing Mineral Resources Development Company Limited*, *Chongqing* 400060, *China*

ABSTRACT: Sedimentary facies is an important factor influencing shale gas accumulation. It not only controlls hydrocarbon generation, but also affects reservoir characteristics and distribution. This paper discusses the Lower Silurian Longmaxi Formation in the south of the Sichuan Basin. Outcrop, core, drilling and logging data identify the sedimentary facies of the formation as continental shelf facies, which is divided into two subfacies: an inner shelf and an outer shelf subfacies. These two subfacies can be further divided into seven microfacies: muddy silty shallow shelf, calcareous silty shallow shelf, muddy limy shallow shelf, storm flow, muddy deep shelf, silty muddy deep shelf and contour current microfacies. Vertical and horizontal distribution of microfacies establishes a sedimentation model of the continental shelf facies. Combined with analization or calculation of geochemical, mineralogical, physical and gas-bearing properties of samples, sedimentary microfacies is evaluated using nine parameters: total organic carbon content, effective shale continuous thickness, vitrinite reflectance, kerogen type, mineral components, porosity, permeability, water saturation and gas content. The evaluation revealed that the most favorable facies for shale gas exploration and development are the muddy deep shelf and part of the silty muddy deep shelf microfacies, with TOC more than 2%, siliceous component over 50%, clay less than 30%, porosity more than 3%, water saturation lower than 40%, gas content greater than 2 m^3/t. These results provide a theoretical basis for deciston-making on the most promising areas for shale gas exploration in the Sichuan Basin and for marine shale gas exploration and development in South China.

KEY WORDS: Sichuan Basin, shale gas, Longmaxi Formation, sedimentary facies, continental shelf.

0 INTRODUCTION

Shale gas is an unconventional hydrocarbon resource, whose gas components are present mainly in free, adsorbed or dissolved states in dark shale (Curtis, 2002). Exploration and development of this type of gas reservoir has received much attention from the central government of China due to energy shortage in China and the rapid development of the shale gas industry in North America. And a mid and long-term development plan has been developed and the Lower Palaeozoic Longmaxi Formation in the Sichuan Basin and adjacent areas has been targeted as an essential area for shale gas exploration (Zou et al., 2013; Editorial Board of Shale Gas Geology, Exploration and Development Practice Collection, 2011). Better understanding of its geological features welt certainly has a profound influence on future progress in exploration and development of shale gas.

Sedimentary facies is one of the most important factors influencing the quality and distribution of hydrocarbon source, reservoir and cap rocks (Bjørlykke, 2014) by its direct impact on organic carbon content, rock components, thickness and distribution; key parameters for evaluating shale gas reservoirs (Zou et al., 2013; Editorial Board of Shale Gas Geology, Exploration and Development Practice Collection, 2011; Gareth and Marc, 2008; Boyer et al., 2006; Montgomery et al., 2005; Pollastro, 2003; Hill et al., 2004; Cluff and Dickerson, 1982; Harris et al., 1978). Dark mudstone or shale is mainly deposited in environments containing low energy and reducing sedimentary environment with abundant organisms in transgression, threshold, stratification and current upwelling sedimentary settings such as swamp, closed bay, lagoon, shelf, continental slope, underfilled basin and deep lake environments (Zou et al., 2013; Aplin and Macquaker, 2011; Potter et al., 2005; Wignall, 1991; Friedman and Sanders, 1978; Picard,

*Corresponding author: wxzswpi@163.com

Manuscript received April 16, 2014.
Manuscript accepted December 20, 2014.

Li, Y. Z., Wang, X. Z., Wu, B., et al., 2016. Sedimentary Facies of Marine Shale Gas Formations in Southern China: The Lower Silurian Longmaxi Formation in the Southern Sichuan Basin. *Journal of Earth Science*, 27(5): 807–822. doi: 10.1007/s12583-015-0592-1. http://en.earth-science.net

1971). Studies of shale gas exploration and development in North America also show that shale gas reservoirs are mainly developed in hypoxic and stagnant depositional environments (Loucks and Ruppel, 2007; Martineau, 2007; Meyers, 2006; Montgomery et al., 2005; Stevenson and Dickerson, 1969) such as the Barnett shale deposited in a hemipelagic hydrostatic deep slope-basin facies and New Albany shale in a deep shelf facies. American studies of the sedimentary environments of shale gas reservoirs have mainly followed a whole environment and lithofacies approach (Abouelresh and Slatt, 2012; Slatt et al., 2012; Hickey and Henk, 2007; Loucks and Ruppel, 2007), and most Chinese studies have similar perspective (Zheng et al., 2013; Liang et al., 2009; Ma et al., 2009) although a few have turned to a lithofacies perspective (Liang et al., 2012). However, all the studies above lack detailed understanding of relationships between the characteristics and distribution of different sedimentary microfacies and the distribution of shale gas reservoirs. Therefore a better understanding about shale gas in a paleogeographic tectonic framework and especially the distribution pattern of sedimentary microfacies, is key to interpreting the distribution of shale gas and of great value for further understanding the characteristics of shale gas reservoirs.

Previous studies indicate that the Lower Paleozoic Longmaxi Formation in the Sichuan Basin and its adjacent areas has good potential for shale gas exploration (Zou et al., 2013, 2010; Jia et al., 2012). Geological investigations of its sedimentary facies have a long history (Dai et al., 2014; Fang et al., 2013; Zheng et al., 2013; Li et al., 2012; Mu C et al., 2011; Zheng and Hu, 2010; Liang et al., 2009, 2008; Ma Y et al., 2009; Chen et al., 2004; Guo et al., 2004; Ma et al., 2004; Bureau of Geology and Mineral Resources of Sichuan Province, 1997, 1991; Liu and Xu, 1994; Zhou et al., 1993; Li, 1991; Zhai and Wang, 1989; Wang, 1985; Mu E et al., 1983). They reveal that in the Early Silurian Period, the Sichuan Basin was a semi-closed restricted marine basin on the upper Yangtze platform caused by accretion and enlargement of the surrounding Leshan-Longnüsi uplift, central Guizhou uplift and ancient West Sichuan Central Yunnan terrain (Zhou et al., 1993; Bureau of Geology and Mineral Resources of Sichuan Province, 1991). Its sedimentary environments have been variously described as a restricted shallow sea (Mu et al., 2011; Wang, 1985), carbonaceous silt lagging platform and calcareous argillo-arenaceous platform (Bureau of Geology and Mineral Resources of Sichuan Province, 1991), shallow water platform (Bureau of Geology and Mineral Resources of Sichuan Province, 1997), stagnant basin or semi-landlocked bay (Li et al., 2012) but the majority current view is that the Longmaxi Formation was deposited in a continental shelf environment (Zheng et al., 2013; Zheng and Hu, 2010; Liang et al., 2009; Ma et al., 2009; Guo et al., 2004; Liu and Xu, 1994; Li, 1991) and this has been tentatively confirmed during later hydrocarbon exploration. These results are preliminary and mainly supported by interpretation of regional geology; so far no detailed research has been carried out into the relationship between the sedimentary facies of Longmaxi Formation in Sichuan Basin and exploration for shale gas. With the progress of exploration and development of shale gas in Sichuan Basin in recent years, significant discoveries have been made in several areas such as Weiyuan, Changning and Fushun-Yongchuan in southern Sichuan, and Fuling and Pengshui in eastern Sichuan. There is an urgent need for accurate research into the geological characteristics of shale-gas rich formations to identify distribution patterns of sedimentary facies to effectively guide exploration and development of shale gas in the Longmaxi Formation.

Our present study establishes a sedimentary model partly built on the work of previous researchers that predicts vertical and horizontal distribution patterns by macroscopic and microscopic observations of outcrops and cores, drilling and logging data combined with observed sedimentary facies types in the Lower Silurian Longmaxi Formation in the southern region of Sichuan Basin. Using this model and relevant data obtained from lab analyses, the relationship between sedimentary facies and shale gas reservoir is explored and sedimentary facies types favorable for shale gas distribution are presented. The authors hope that the results of this research could provide a theoretical basis that can be used to identify optimal shale gas exploration in Sichuan Basin and will be useful for the exploration and development of marine shale gas in a wider region of South China.

1 GEOLOGICAL BACKGROUND

The region of interest is located in the southern Sichuan Basin on the northwest edge of the upper Yangtze platform. Its geographic range roughly covers a total area of about 5×10^4 km^2 region containing Emeishan in the west, the Qijiang District of Chongqing in the east, Ziyang-Hechuan in the north, and Bijie of Guizhou in the south (Fig. 1). The region is crossed by the Northeast-Southwest Huaying Mountain-Qingshanling fault zone, North-South Changshou-Zunyi fault zone, and the East-West Gulin-Yanjin fault zone in the south (Fig. 1). Discontinuous folding structures predominate along the edge of southern Sichuan with a linear arrangement of southern Sichuan trending northeast-southwest. The main tectonic structures are the Weiyuan structure, Yanggaosi structure and Changning structure (Liu et al., 2012; Zhai and Wang, 1989).

The Lower Silurian Longmaxi Formation was deposited during the Rhuddanian and Aeronian stages of the Silurian system (Lin et al., 1998). In the Sichuan Basin and surrounding areas the Longmaxi Formation is mainly composed of two sedimentary cycles which are composed of a set of black, gray-black (silty) mudstone and/or shale, gray and dark-gray siltstone, and subordinate gray to dark gray carbonate rocks (Fig. 2). The darker intervals at the bottom of each cycle are rich in carbonaceous rocks with a high TOC and a certain amount of pyrite. The formation reaches its greatest thickness in southern Sichuan, eastern Chongqing, western Hubei and northern Sichuan (Lin et al., 1998). A total or partial break in the succession occurs near ancient uplifts and in the western part of the basin (Lin et al., 1998). The middle and especially the lower stratum of the strata is rich in graptolites, mainly *Glyptograptus persculptus*, *Pristiograptus cyphus*, *Demirastrites triangulatus*, *Monograptus sedgwickii* and *Spirograptus turriculata* among other species, with other fossils including brachiopods and cephalopods fossils. The Longmaxi Formation has a conformable contact with underlying strata of

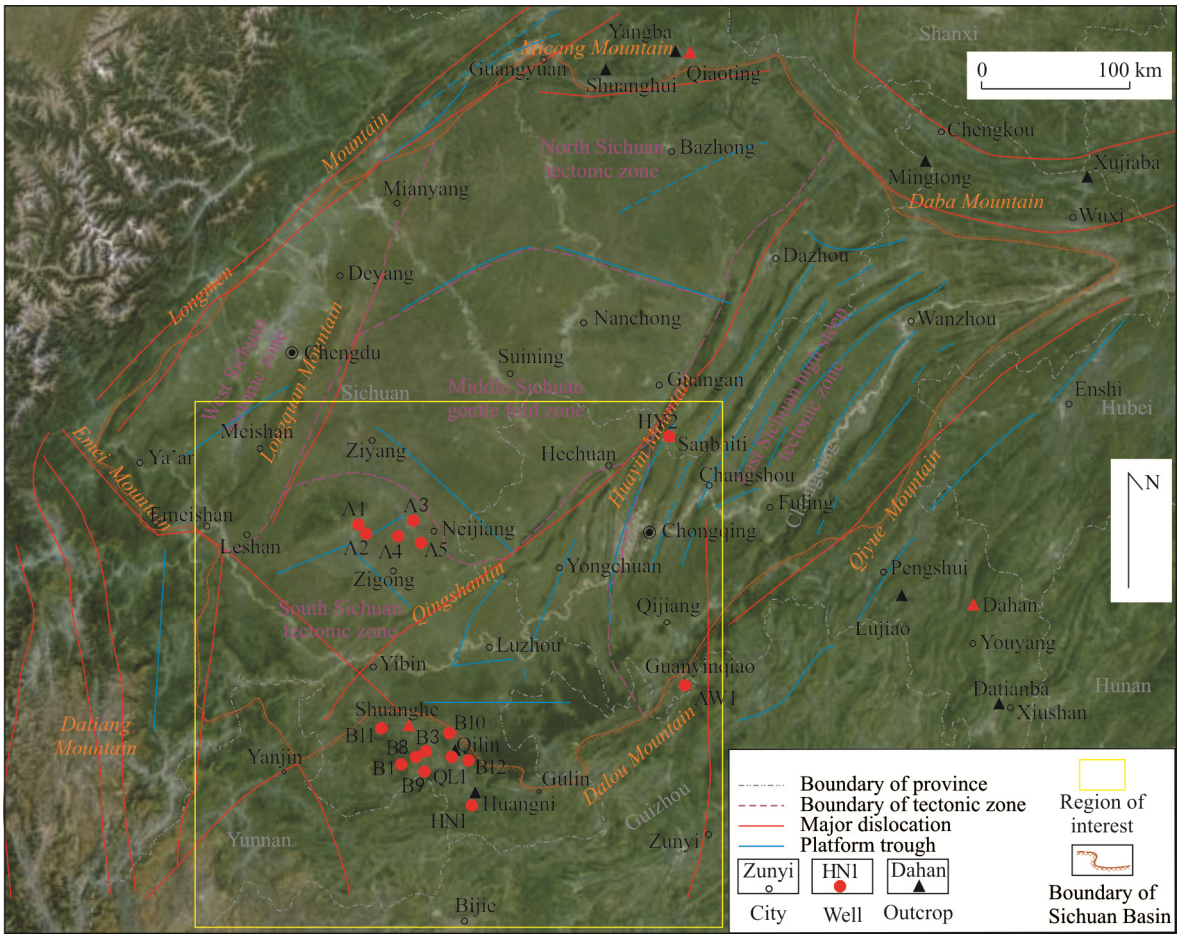

Figure 1. Topographic map of Sichuan Basin, showing the main tectonic structure and zones, the location of interest in the region, the field outcrops and sample resources (red pots and triangles).

the Upper Ordovician Wufeng Formation but due to the impact of surrounding ancient uplifts and land, unconformable contacts with overlying strata are different in different locations, like the Lower Permian Liangshan Formation in the north and the Lower Silurian Shiniulan Formation within the region in the south.

2 METHODOLOGY

Macroscopic and microscopic observation of 13 outcrops and more than 20 well cores, analysis of drilling and logging data in South Sichuan and adjacent areas (Fig. 1), lithological, paleontological, electrical and other properties reflecting sedimentary environments were combined with previous stratigraphic, paleontological and sedimentary research (Dai et al., 2014; Fang et al., 2013; Zheng et al., 2013; Li et al., 2012; Mu C et al., 2011; Zheng and Hu, 2010; Liang et al., 2009, 2008; Ma et al., 2009; Chen et al., 2004; Guo et al., 2004; Bureau of Geology and Mineral Resources of Sichuan Province, 1997, 1991; Liu and Xu, 1994; Zhou et al., 1993; Li, 1991; Zhai and Wang, 1989; Wang, 1985; Mu E et al., 1983) to arrive at a classification scheme and model of sedimentary facies in the region of interest. Nine parameters based on shale gas geological research conducted in China and abroad (Guo et al., 2011; Sondergeld et al., 2010; Jenkins and Boyer, 2008; Bowker, 2007, 2003; Jarvie et al., 2007, 2004; Boyer et al., 2006; Curtis, 2002) were selected to test the quality of shale gas reservoirs (Table 1): (a) total organic carbon content (TOC), (b) effective shale continuous thickness (H), (c) kerogen type, (d) vitrinite reflectance (Ro), (e) mineral components, (f) porosity (Φ), (g) permeability (K), (h) water saturation (S_w) and (i) gas content (G).

Data from over 2 000 samples obtained from outcrops and drill cores were obtained in two ways. About 1 800 samples were provided by PetroChina Southwest Oil and Gas Field Company, along with a complete set of analysis data of conventional physical properties and gas content. The other data from more than 300 samples were collected from four outcrops and drilling cores of several wells and analyzed in accordance with Chinese Petroleum Industry Standards SY/T 5125-1996; GB/T 19145-2003; SY/T 5163-2010; SY/T 5124-2012; and SY/T 6940-2013 (Committee of Petroleum Geology Exploration of Professional Standards, 2013, 2012, 2010, 2003, 1996) at the State Key Laboratory of Oil and Gas Reservoir Geology and Exploitation in Southwest Petroleum University and the Analysis and Test Center for Exploration and Development Research Institute of the PetroChina Southwest Oil and Gas Field Company.

The parameters were obtained as follows: TOC, according to GB/T 19145-2003 (Committee of Petroleum Geology Exploration of Professional Standards, 2003), samples from

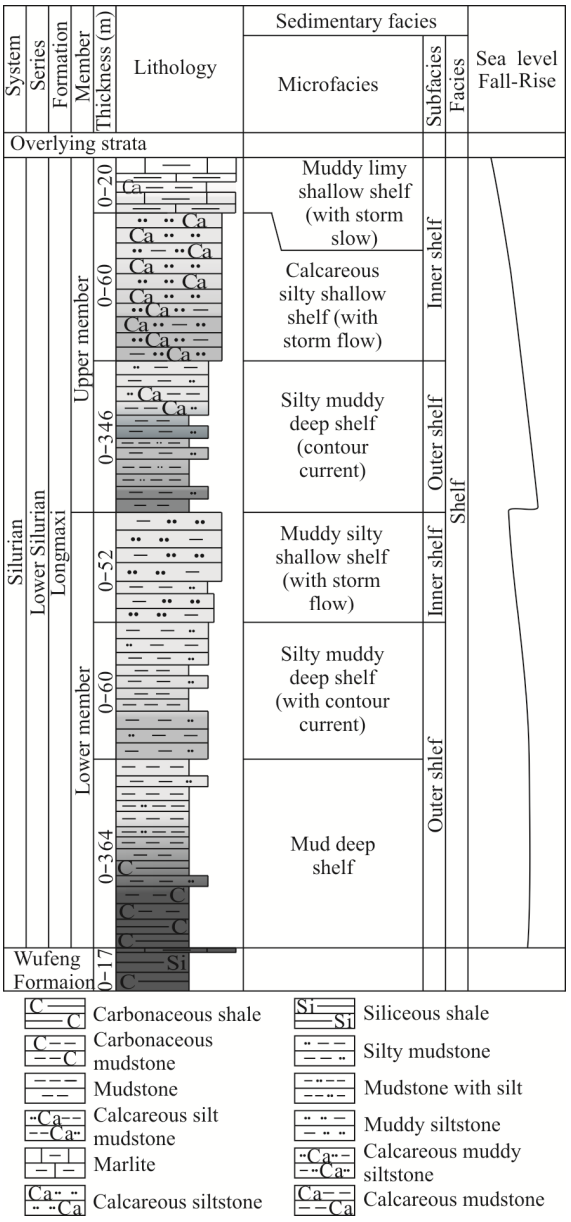

Figure 2. Stratigraphy and sedimentary facies of Longmaxi Formation in the region of interest.

drill cores from 12 wells: AW1, HY2, HN1, QL1, A1, A2, A3, B1, B3, B8, B10, and B11; and 4 outcrops: Shuanghe, Sanbaiti, Dahan, and Qiaoting were analyzed using a CS-400 carbon-sulfur analyzer at a temperature of 30 ºC and a humidity of 65% RH. *H* was determined as the continuous stratigraphic thickness over which TOC≥2% from stratal thickness and TOC measurements. Because the Longmaxi Formation is marine and vitrinite measurements were not available, *R*o was determined from the reflectance of bitumen (Ro_b) (Whelan and Thompson-Rizer, 1993; Xiao et al., 1991; Gentzis and Goodarzi, 1990; Feng and Chen, 1988) from drill cores of 6 wells, AW1, HY2, HN1, QL1, A1, B1, and B3; and 4 outcrops, Shuanghe, Sanbaiti, Dahan, and Qiaoting. The formula Ro=0.679 0 Ro_b+0.319 5 (Feng and Chen, 1988) was chosen, Ro_b was measured by micro-photometer at a temperature of 21 ºC and a humidity of 60% RH according to (SY/T 5124-2012). Macerals of kerogen

Table 1 Evaluation parameters of shale gas reservoir (modified from Sondergeld et al., 2010; Boyer et al., 2006)

TOC	>2.0%
Effective shale continuous thickness	>30 m
*R*o	>1.4%
Kerogen types	Ⅰ or Ⅱ$_1$
Mineral components	Siliceous components >40%
	Clay <30%
Porosity	>3%
Permeability	>100 nd
Water saturation	<40%
Gas content	2 m^3/t

in samples from drill cores of 6 wells, AW1, HY2, QL1, A1, B1, and B3 were directly analyzed with a transmitted light microscope at a temperature of 22 ºC and a humidity of 60% RH according to (SY/T 5125-1996) to identify kerogen type; and organic matter classified into three categories and four types. The formula TI=(a×100+b×50-c×75-d×100)/100 where a, b, c and d stand for the percentage of sapropelinite, liptinite, vitrinite and inertinite respectively, was used to calculate a weighted type index TI to determine kerogen type. Mineral components of samples from drill cores of 7 wells, AW1, HY2, HN1, QL1, A1, B1, and B3, and 4 outcrops, Shuanghe, Sanbaiti, Dahan, and Qiaoting, were analyzed according to SY/T 5163-2010 by X' Pert PRO X-ray diffraction over a temperature range of 15–25 ºC and humidity ≤70% RH. Φ, K and S_w were measured directly using samples obtained from drill cores of 4 wells, A1, B1, B3, and B12, using a high-pressure drill core gas logging permeameter at an ambient temperature of 20–30 ºC and conventional analysis methods. The total gas content of samples from drill cores of two wells, A1 and B1 was measured using a desorption method according to (SY/T 6940-2013) as the sum of measured gas content, lost gas content and crushed gas content.

The sedimentary microfacies most favorable for shale gas exploration based on all the research work above was finally screened out by analyzing the relationship between microfacies and shale gas reservoirs.

3 RESULTS

3.1 Lithological Characteristics

The lithology of the lower part of the Longmaxi Formation is dominated by lamellar or massive, black or gray-black mudstones, carbonaceous shale (Figs. 3a, 3b, 4a, 5a) and dark gray silty mudstones and/or shale (Figs. 3c, 4b), with locally imbedded gray-green or dark gray argillaceous siltstones (Fig. 3e) and calcareous siltstones. The lithology of the upper part is dominated by dark gray or grayish-green silty mudstones (Fig. 3d), calcareous mudstones and light gray argillaceous siltstones (Figs. 3f, 5b), marls, limestones, etc.. Light gray-gray tempestites (Fig. 4c) and contourites (Fig. 4d) are imbedded locally in these horizons, with abundant pyrites with nodular (Fig. 4a), dispersed (Fig. 5a), crack-filling and framboidal shapes. The first two shapes are found especially in dark intervals among fine grained rocks.

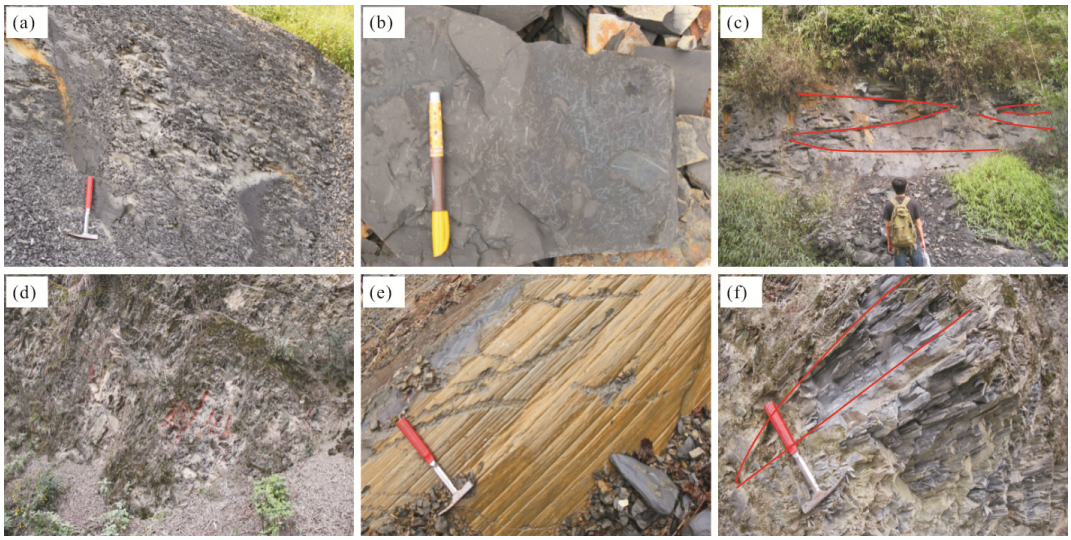

Figure 3. Outcrop photos. (a) Black shale, horizontal bedding, Shuanghe; (b) abundant graptolites, Dahan; (c) dark gray to grayish black silty mudstone, massive bedding and wedge-shaped cross bedding, Shuanghe; (d) gray-green silty shale, cross bedding, Sanbaiti; (e) gray green muddy siltstone, massive bedding, weathering to yellow and yellow green in joints, Lujiao; (f) gray green muddy siltstone, hummocky cross-bedding, Sanbaiti.

3.2 Sedimentary Structures

Horizontal massive bedding is the most common sedimentary structure in the region. Horizontal bedding appears most frequently in fine silty argillaceous sediments (Figs. 3a, 3d, 4a). Massive bedding can be found both in fine and coarse sediment. Homogeneous, non-sorted laminated, black, massive bedding is always found on a large scale in shale or dark gray to grayish green argillaceous siltstone as layers ten centimeters to several meters thick (Figs. 3c, 3e). Bedding in siltstone and marl is thinner, and original bedding may have been destroyed or disturbed by a large number of benthonic organisms.

Rhythmic layering, graded bedding, directional ripple bedding and cross bedding are uncommon. Rhythmic layering (Fig. 4b) is found mostly in the northern part of the region. Graded bedding (Fig. 4c) is mainly formed from storm deposit with layers of several to dozens of centimeters thick with positive grain-size gradation. Directional ripple bedding (Fig. 4d) is found in contourites, mainly developed in gray-white argillaceous calcareous siltstone, which often embedded in large bodies of dark shale as moderately thick to thin sheets or lenses. Wedge-shaped cross bedding (Fig. 3c) and hummocky cross bedding (Fig. 3f) are both present in light-colored beds. Wedge-shaped cross bedding appears on a large scale as single beds dozens of centimeters thick; while hummocky cross beds, the result of storm action, range in thickness from several centimeters to dozens of centimeters, and can be classified as tempestites.

Other special sedimentary structures also occur, such as lenticular structure, erosion surfaces and bioturbation structures. Lenticular structures with a lenticular or bean-shape (Fig. 4e) are mostly found in the upper part of the Longmaxi Formation in the south. The “beans” are arranged intermittently in strings composed of lighter colored calcareous siltstone or micrite. The “bean skin” is composed of darker argillaceous siltstone, silty mudstone or marl, and its bedding is not apparent. The lenticular structure was caused by storm action and later uneven compaction. Associated erosion surfaces (Figs. 4c, 4d) are above or below tempestite or contourite beds indicating storm flow and contour flow. Penecontemporaneous storm flow or storm waves agitated early unconsolidated or semi-consolidated sediments including continental shelf mud, resulting in erosion surfaces with gullies, flutes and tool marks. Straight tube-shaped burrow structures (Fig. 4f) and irregular patchy disturbances of various grain sizes and colors (Fig. 4g) concomitant with tempestite are often found in drill cores.

3.3 Paleontology

Many fossils occur in outcrops and the drill cores. Graptolites are most abundant in black shale (Figs. 3b, 4h), and the most common are the species of *Climacograptus*, *Glyptograptus*, *Pristiograptus*, and *Rastrites*. Radiolarians, sponges and cephalopods are second in abundance. Radiolarians and sponge spicules can be observed in the thin sections (Figs. 5c, 5d), and sponges and cephalopods often found together with graptolites (Figs. 4i, 4h). There are relatively few brachiopods (Fig. 4k), gastropods (Fig. 4l), ostracods (Fig. 5e), crinoids (Fig. 5f) and trilobites, with the first three categories featuring small individuals and thin shells.

3.4 Sample Data

The samples were tested and analyzed in the laboratory to obtain the nine parameters based on measurements and calculations previously outlined in the text and Table 1, with the following results.

(a) TOC: 2 091 samples; values range from 0.06% to 9.91%, average 1.15%; 62.7% of samples have a value greater than 0.5%, 2% of samples exceed 17.3% (Fig. 6a); every well has a high average value from 0.71% to 2.87%.

(b) *H*: values range from 0 to 41 m, mainly in the Lower Member of the Longmaxi Formation.

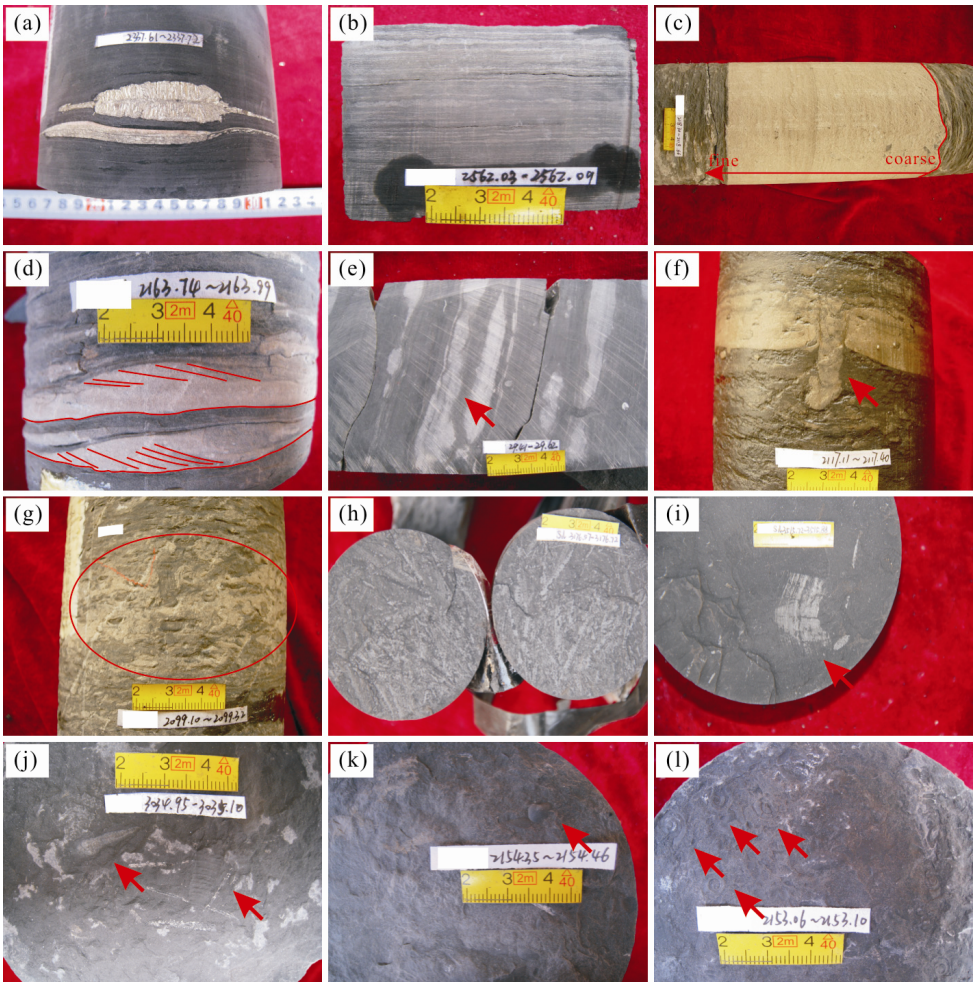

Figure 4. Photos of cores. (a) Grayish black shale, horizontal bedding, nodular pyrite, Well B11, 2 337.61–2 337.72 m; (b) gray black silty mudstone and grey muddy siltstone, rhythmic layering, Well A2, 2 562.03–2 562.09 m; (c) tempestite, massive bedding, with erosion surface and positive grading, Well B3, 2 118.30–2 118.66 m; (d) contourite, directive ripple lamination and erosion surface, Well B3, 2 163.74–2 163.99 m; (e) black calcareous mudstone and lenticular gray white marl, lenticular structure, Well QL1, 29.41–29.62 m; (f) burrow, Well B3; (g) bioturbation structures including a burrow, Well B3, 2 099.10–2 099.32 m; (h) abundant graptolite fossils, Well A3, 3 176.57–3 176.72 m; (i) sponge fragments, Well A4, 3 515.72–3 515.88 m; (j) cephalopods, Well B9, 3 034.95–3 035.1 m; (k) brachiopods, Well B3, 2 154.35–2 154.46 m; (l) gastropods, Well B3, 2 153.06–2 153.10 m.

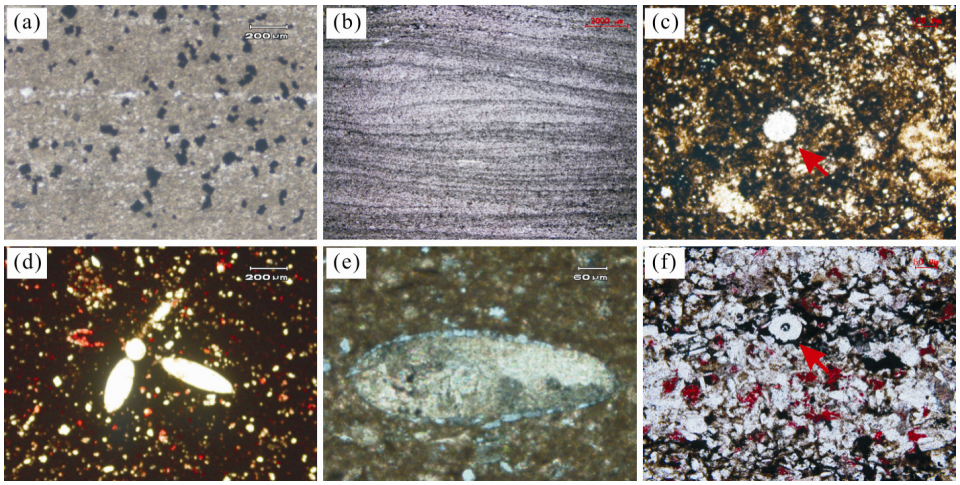

Figure 5. Photos of thin sections. (a) Dispersed pyrites, Well A1, 1 382.24–1 382.32 m, 10×4(-); (b) muddy siltstone, 10(-), hummocky cross bedding, Dahan; (c) radiolarian, Qiaoting, 10×4(-); (d) Well B1, 2 509.91–2 509.94 m, 10×4(-), siliceous sponge spicules; (e) ostracods, Well B3, 2 187.44–2 187.47 m, 10×10 (+); (f) echinoderm debris, Dahan, 10×10(-).

(c) *R*o: 93 samples; values range from 1.75% to 2.87%, average 2.4%; 69.5% samples have a value between 1.8% and 2.2% (Fig. 6b); every well has a high average value from 1.81% to 2.7%.

(d) Kerogen type: 93 samples; TI values range from 56.2 to 93, average 80.2, 67.7% samples have a value greater than 80 (Fig. 6c); most samples are Type I, while a small number are Type II_1.

(e) Mineral components: 963 samples; clay minerals, illite, illite/smectite, kaolinite and chlorite from 0 to 75.9%, average 27.5%, 7.4% are between 20% to 40%; quartz, feldspar and pyrite range from 4.9% to 93.4%, mainly between 20% to 80%, average 48.3%; calcareous components calcite, dolomite and siderite, range from 0 to 87.2%, average of 24.2%, 93.0% of which are less than 50% (Fig. 6d).

(f) Φ: 479 samples; values rather low ranging from 0.7% to 10.27% average 3.2%, 85.0% between 1% and 6% (Fig. 6e);

(g) *K*: 244 samples; values rather low, ranging from 5.55 to 18.7×10^6 nD, average of 2.12×10^6 nD, 75% are between 10^4 to 10^6 nD (Fig. 6f).

(h) S_w: 479 samples; values range from 14.6% to 98.8% with average 54.6%, 79.8% greater than 30% and 61.4% are between 30% to 60% (Fig. 6g).

(i) *G*: 36 samples; values range from 0.29 to 5.01 m^3/t average 1.72 m^3/t (Fig. 6h); measured gas content values range from 0.05 to 1.09 m^3/t average 0.56 m^3/t; crushed gas content values range from 0.22 to 1.70 m^3/t, average 0.87 m^3/t; lost gas content values range from 0.08 to 2.21 m^3/t, average 0.40 m^3/t.

4 DISCUSSION

4.1 Classification of Sedimentary Facies

Our lithological, sedimentary and paleontological characteristics indicate that the southern region of Sichuan Basin was in a continental shelf environment with deep water, low-energy, oxygen-poor and strong reduction in the period of deposition of the Longmaxi Formation. Most previous studies of sedimentary facies in the region focused on the division and characteristics of subfacies (Zheng et al., 2013; Zheng and Hu, 2010; Ma et al., 2009; Liu and Xu, 1994) rather than explanations of differences between subfacies although a small number of researchers have studied sedimentary subfacies and microfacies (Liang et al., 2009; Guo et al., 2004). Some of their microfacies have similar names and their characteristics are hard to distinguish, e.g., "argillaceous shallow shelf" and "argillaceous deep shelf" (Guo et al., 2004), could have developed in other sedimentary environments such as turbidity currents at slope breaks (Guo et al., 2004), or should have been classified as biofacies rather than sedimentary facies (Liang et al., 2009). All such classification schemes have turned out to be hard to use in shale gas exploration. In this paper we have interpreted and defined the sedimentary facies in the southern region of Sichuan Basin using abundant data and precisely defined parameters and established a new classification scheme that fits the Longmaxi Formation, based on characteristics such as sediment type,

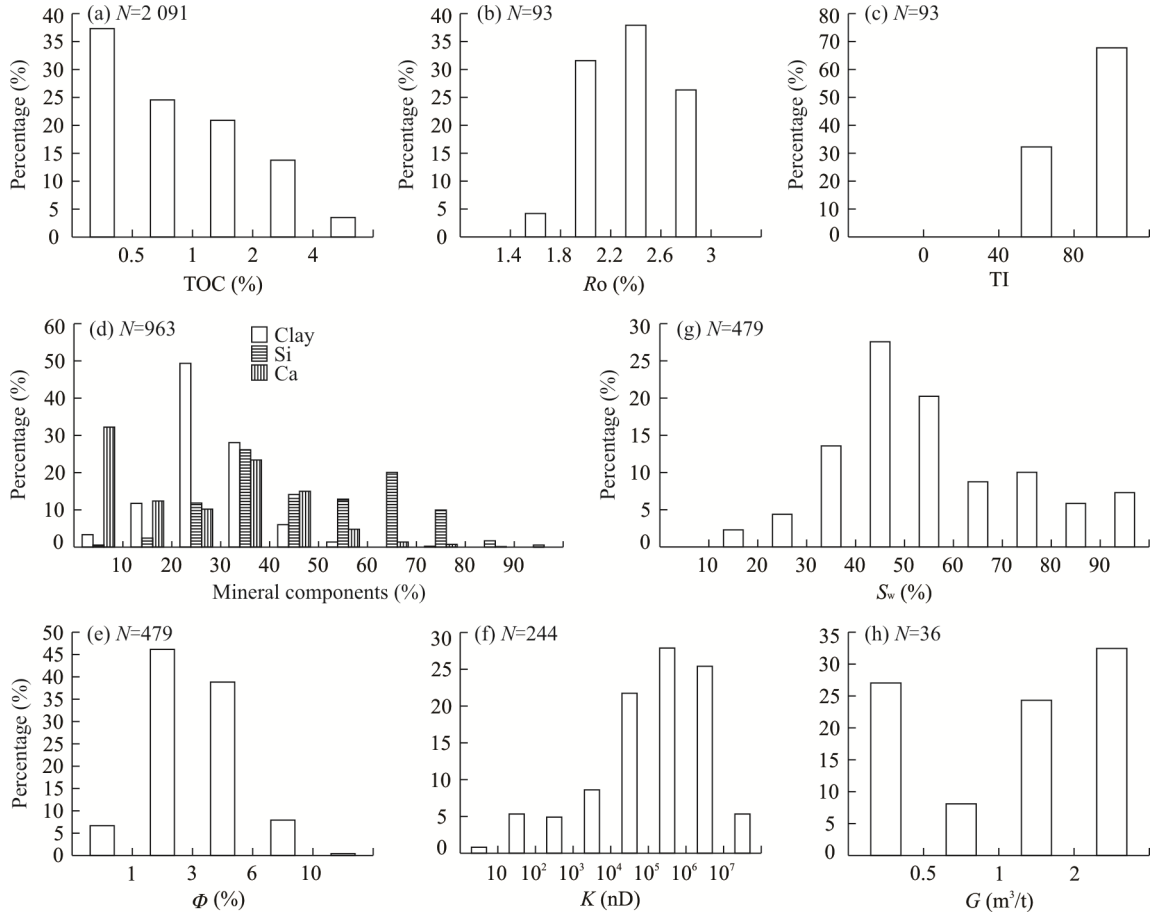

Figure 6. Bar charts of sample data distribution bar charts. (a) TOC; (b) *R*o; (c) TI; (d) mineral components; (e) Φ; (f) *K*; (g) S_w; (h) *G*.

fossils, electrical and other properties. The shelf facies of the Longmaxi Formation has been divided into two subfacies: an inner shelf and an outer Shelf subfacies, which are further divided into seven microfacies. All these sedimentary microfacies are either named after their primary rock type and water depth, e.g., silty muddy deep shelf microfacies, or after their dominant mode of genesis, e.g., contour current Microfacies. Details of the classification follow.

4.1.1 Inner shelf subfacies

The inner shelf subfacies was located between normal wave base and normal storm wave base in shallow water between 20 and 50 m. This was an environment with relatively high energy, influenced and changed by intermittent storm flow, tidal and ocean currents. Its predominant lithologies are siltites and carbonates with subordinate relatively low energy lamellar mudstones and shales. Sedimentary structures include massive bedding, graded bedding and lenticular structures, and bioturbation structures are frequently present. Fragments of fossils such as echinoderms, trilobites, brachiopods and foraminifers are frequently observed, with smaller amounts of ostracods, sponge spicules and graptolites. The inner shelf subfacies incorporates the muddy silty shallow shelf, calcareous silty shallow shelf, muddy limy shallow shelf and storm flow microfacies.

The lithology of the muddy silty shallow shelf microfacies (Fig. 7a) is predominately gray to dark gray argillaceous siltstone containing a small amount of dark gray silty mudstone, gray to dark gray calcareous argillaceous siltstone or calcareous siltstone. Predominant sedimentary structures are massive bedding and rhythmic layering, with occasional horizontal bedding, erosion surfaces and local graded bedding. A small amount of fossils are generally broken, with common echinoderms, trilobites, foraminifers, and brachiopods, and occasional graptolites. There is a small amount of nodular pyrite. Natural gamma (GR) values range medium to low with large amplitude, often from 80 to 120 API.

The lithology of the calcareous silty shallow shelf microfacies (Figs. 7b, 8) is predominately gray to dark gray calcareous siltstone containing a small amount of dark gray to grayish-black calcareous mudstone, gray to dark gray argillaceous siltstone or argillaceous calcareous siltstone. Predominant sedimentary structures are massive bedding and rhythmic layering, with occasional cross bedding, erosion surface and bioturbation structures. Incomplete fossils of echinoderms, trilobites, foraminifers, brachiopods and gastropods are infrequently observed, and more rarely graptolites. GR values range from medium to low, lower than those of the Muddy Silty Shelf microfacies, with large amplitude, frequently from 40 to 120 API.

There are three possible reasons for the changes in the argillaceous sediment content and the calcareous sediment content in these two microfacies: (a) their different provenances, the muddy silty shallow shelf microfacies was near the sediment source and had a higher argillaceous sediment content and lower calcareous sediment content in contrast to the the conditions for the calcareous silty shallow shelf microfacies; (b) contrasting changes in sedimentary environment due to frequent eustatic sea level changes, carbonate deposition occurred during clear water periods while deposition of fine-grain detrital materials of terrigenous origin occurred during muddy water periods; (c) diagenesis accompanied by metasomatism, chemical and biochemical action: This may have also given rise to calcareous sediments. In the last case, sediment type should not be considered in facies classification.

The muddy limy shallow shelf microfacies (Fig. 7c) was deposited in an oxidation-reduction zone near the shoreline where the water body was relatively deep, with lower energy and less susceptible to storm flow. The predominant lithology is gray, dark gray and grayish-white marl, argillaceous limestone and calcareous mudstone with lenticular structures, massive bedding and erosion surfaces with occasional incomplete fossils observed and no pyrite content. GR values are low: 20 to 50 API, with a saw-tooth wave distribution. These characteristics indicate that changes of lithofacies in the muddy limy shallow shelf microfacies were affected not only by frequent changes in depth, but also by sedimentation events such as storm flows, or flows of detrital terrigenous materials from shoreside facies into limy sediments, causing inter-mingling of sedimentary components.

The storm flow microfacies (Fig. 7d) is observed in drill cores as single layers ranging from a few centimeters to tens of centimeters thick predominately composed of gray or dark gray high maturity argillaceous siltstone and siltstone. The bedding sequence is generally graded vertically upwards, with normal graded bedding, erosion surfaces and bioturbation structures as well as burrows and escape traces. There is only a small amount of fossils that are relatively incomplete and contain no pyrite, or none. Tempestites are often developed locally interbedded within other inner continental shelf microfacies.

4.1.2 Outer shelf subfacies

The outer shelf subfacies was located below storm wave base and above the continental slope, the water was rather deep at about 50 to 200 m and with relatively low energy. The sediments are mostly fine grained mudstone (shale) predominantly with horizontal bedding and massive bedding. Fossils are mainly graptolites and sponges, with some radiolarians and cephalopods and a few trilobites, brachiopods, ostracods and echinoderms. The outer shelf subfacies incorporates three microfacies: muddy deep shelf, silty muddy deep shelf and contour current microfacies.

The predominant lithology of the muddy deep shelf microfacies (Figs. 7e, 8) is black lamellar or massive (carbonaceous) mudstone (shale) containing a small amount of dark gray silty mudstone (shale), the finest-grained rock type. Predominant sedimentary structures are horizontal bedding with occasional massive bedding. The muddy deep shelf microfacies is often rich in graptolites, sponges and radiolarians with a few ostracods. Nodular and dispersed pyrites is abundant. GR values are the highest in the region, mostly greater than 200 API on a stable curve.

The sediments of the silty muddy deep shelf microfacies (Figs. 7f, 8) have a higher silty component, generally 20%–40%. Massive gray-black silty mudstone accounts for a large proportion while grayish-black lamellar silty mudstone

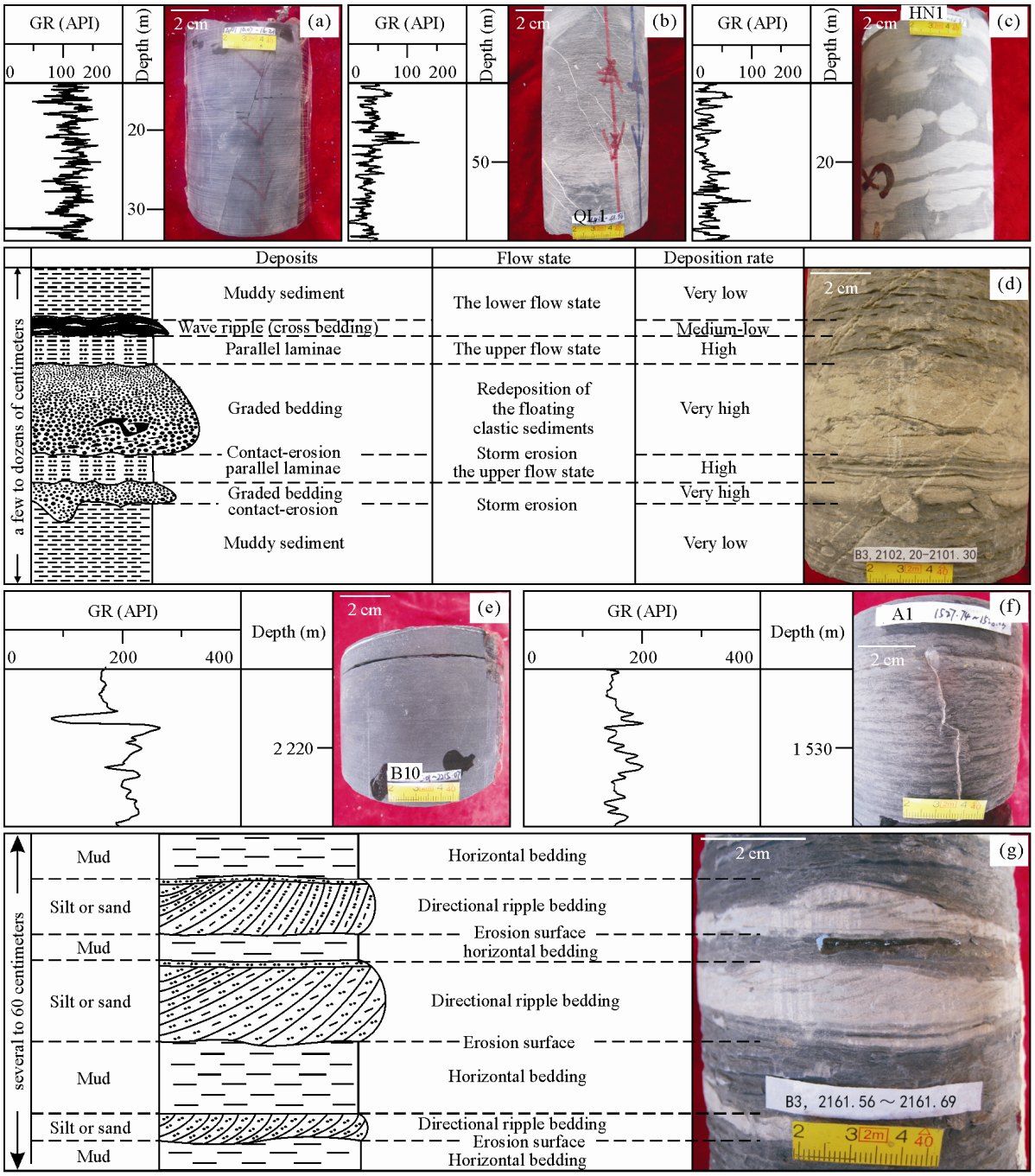

Figure 7. Schematics of various sedimentary microfacies. (a) Muddy silty shallow shelf microfacies; (b) calcareous silty shallow shelf microfacies; (c) muddy limy shallow shelf microfacies; (d) storm flow microfacies; (e) muddy deep shelf microfacies; (f) silty muddy deep shelf microfacies; (g) contour current microfacies.

with interbedded sheet-like and lenticular dark gray carbonates and black mudstone accounts for a smaller portion. Predominant sedimentary structures are cross bedding and massive bedding, with occasional presence of rhythmic layering. The sediments contain large numbers of graptolites and sponges and fewer ostracods and cephalopods. Much nodular and dispersed pyrite is present. GR values range from medium to high amplitude, mostly between 120 and 200 API, presenting a sawtooth curve. The sedimentation of both the muddy deep shelf and silty muddy deep shelf microfacies was extremely undisturbed, indicating a low-energy, oxygen-poor, low-velocity, under-compensated deep water sedimentary environment.

Beds of the contour current microfacies (Fig. 7g) are a few centimeters to tens of centimeters thick, with predominant gray argillaceous siltstone or siltstone with irregular and lamellar or lenticular structures. Directional ripple bedding and erosion surfaces were mainly developed with occasional bioturbation containing a small amount of fossils that are relatively incomplete or none and no pyrite. It often occurs within the muddy deep shelf or silty muddy deep shelf microfacies.

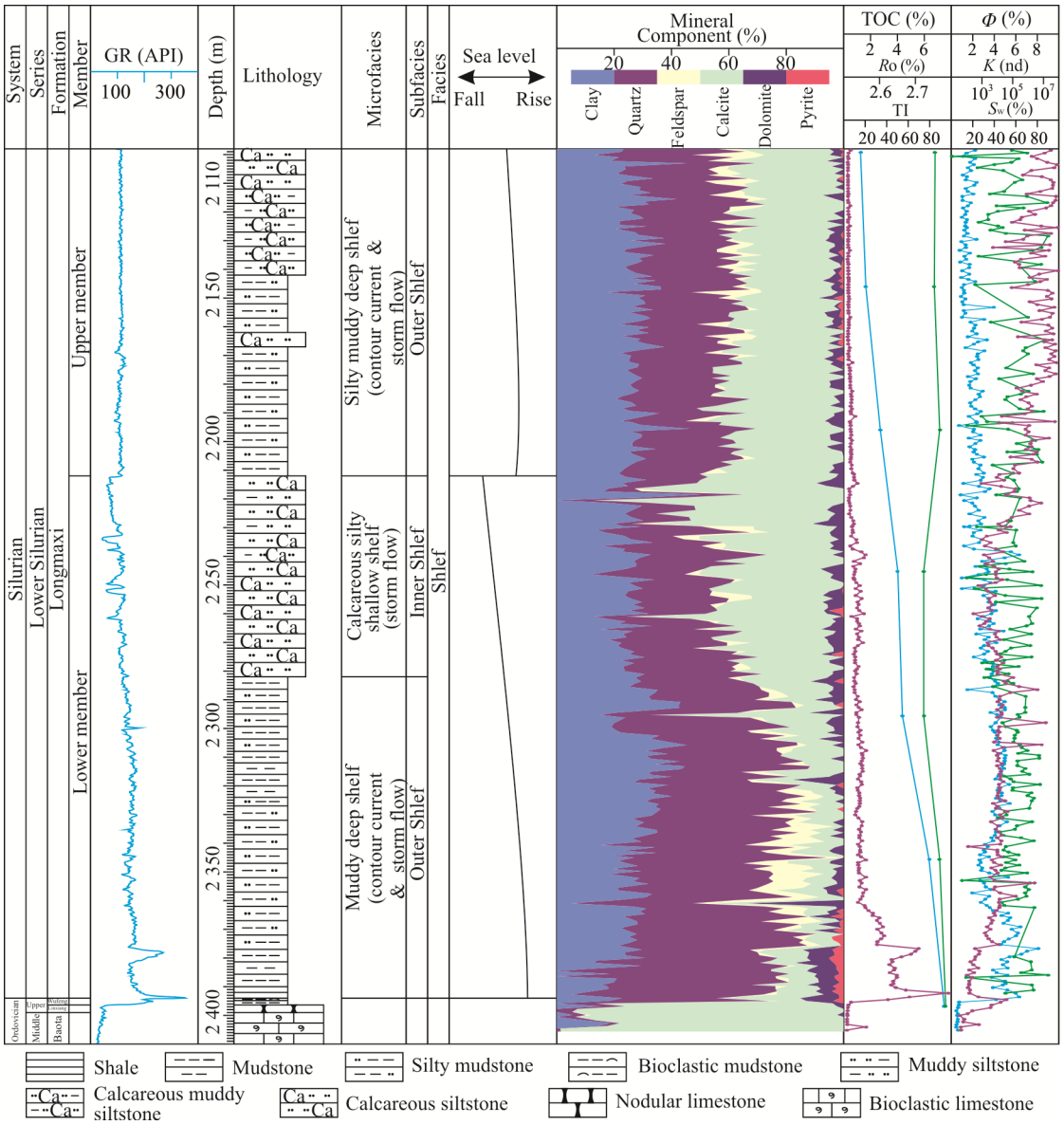

Figure 8. Stratigraphy, sedimentary facies, and sample data of a core section of Well B3.

4.2 Vertical and Horizontal Distribution and Sedimentation Models of Facies

The authors conclude that the region was in a major decline phase of a Class 3 sea level change cycle containing two lower Class 4 cycles of sea level change by studying lithology, electrical properties and sedimentary facies. In onder to identify cycles of sea level change, the author uses data obtained from more than 10 outcrops and almost 30 wells in the southern Sichuan Basin and adjacent areas (Figs. 8, 9) combined with regional geological and global sea level change data during the period of deposition of the Longmaxi Formation (Slatt and Rodriguez, 2012; Mu C et al., 2011; Loydell, 1998; Mu E et al., 1986). Each Class 4 cycle of sea level change began with a rapid marine transgression and ended with a slow marine regression to form two sedimentary cycles (Figs. 2, 9). The transgression in the earlier part of first cycle was due to the end of glacial events in the Late Ordovician. Sea level rose rapidly in the region and the outer shelf subfacies developed, including the muddy deep shelf and silty muddy deep shelf microfacies while the inner shelf subfacies including muddy silty shallow shelf microfacies developed locally near ancient uplifts at the northern and southern edges of the South Sichuan Basin. Sea level fell slowly and the water gradually became shallow in the later part of first cycle. The area of outer shelf subfacies gradually reduced and was eventually confined to a sedimentary sag in the middle of South Sichuan Basin. The inner shelf subfacies mainly including muddy silty shallow shelf microfacies developed and predominated in most of the area. With another rapid transgression at the beginning of the second cycle, the water body became deeper again and the outer shelf subfacies expanded. The second transgression was on a smaller scale than the first, so the silty muddy deep shelf

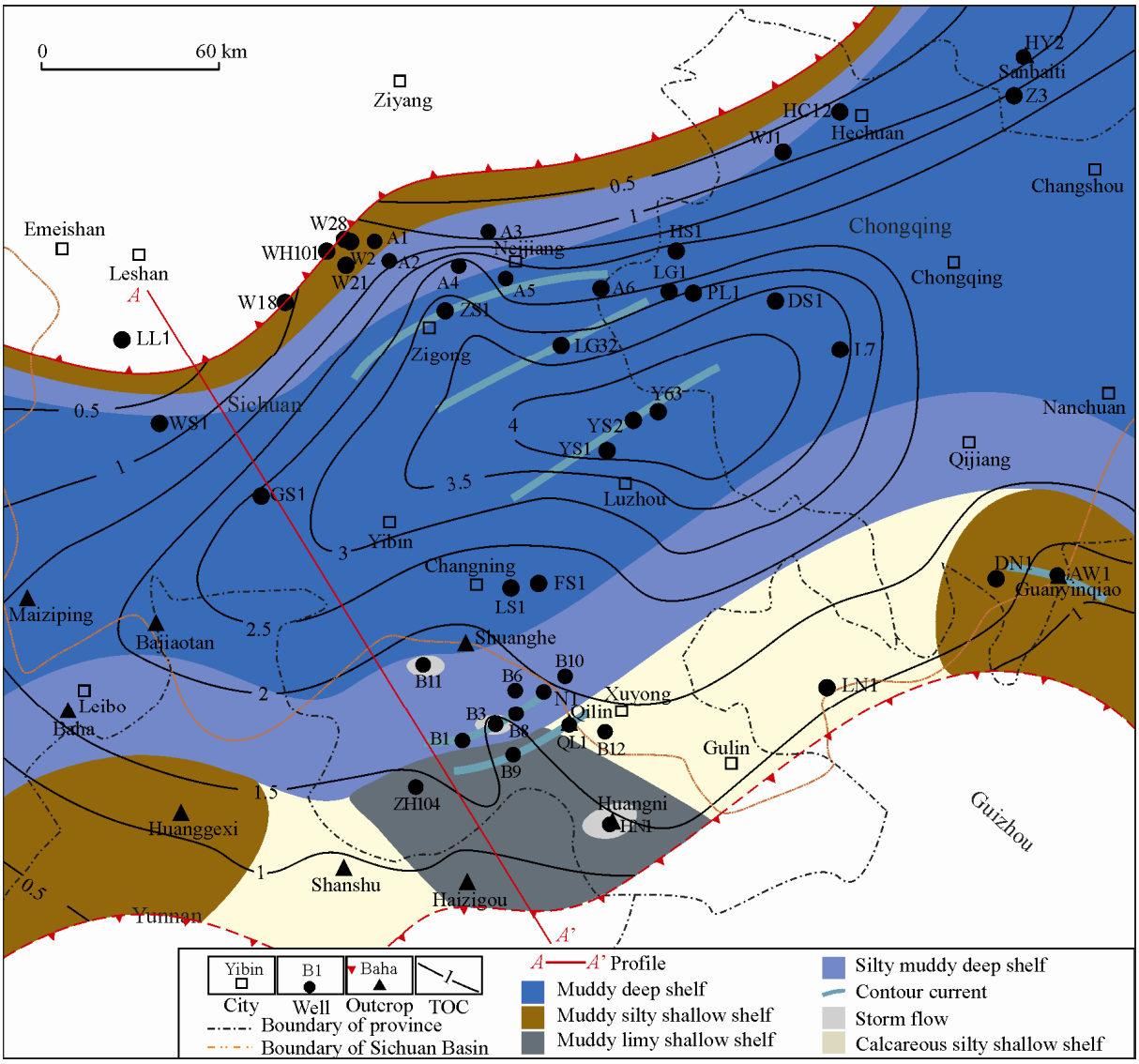

Figure 9. Sedimentary facies distribution map during deposition of the Longmaxi Formation. Wells and outcrops indicated in the map used to identify sedimentary facies.

microfacies predominated, while the muddy deep shelf microfacies only developed in the middle of the South Sichuan Basin and the muddy silty shallow shelf microfacies at the northern edge differed from the calcareous silty shallow shelf microfacies at the southern edge. Sea level fell during the later part of second cycle, and the inner shelf subfacies mainly developed, while the muddy silty shallow shelf microfacies predominated in the northern region and the calcareous silty shallow shelf and muddy limy shallow shelf predominated in the south. The muddy deep shelf and silty muddy deep shelf microfacies occurred locally in the middle of the South Sichuan Basin at that time.

Due to the surface layout of the the central Guizhou uplift and West Sichuan-Central Yunnan paleocontinent created by the Leshan-Longnüsi uplift during deposition of the Longmaxi Formation, sedimentation assemblages developed along a northwest-southeast direction, first the inner, then the outer, last the inner shelf subfacies. The micorfacies appeared in the following order: muddy silty shallow shelf, silty muddy deep shelf, muddy deep shelf, silty muddy deep shelf, calcareous silty shallow shelf (muddy limy shallow shelf, muddy silty shallow shelf) (Figs. 9, 10). The sedimentary environment can be summarized as one depression between two uplifts (Fig. 10).

4.3 Relationship between Sedimentary Facies and Shale Gas Reservoirs

Measured and calculated evaluation parameters combined with sedimentary microfacies indicate as following (Table 2, Fig. 8).

(a) TOC average values of most microfacies are greater than 0.5%, showing that good sources of hydrocarbon were deposited in all microfacies; TOC of outer shelf is generally higher than that of inner shelf, above all the TOC average value of the muddy deep shelf microfacies reaches 2.35%.

(b) The effective shale continuous thickness is greatest in the silty muddy deep shelf and muddy deep shelf microfacies, up to 30 m at some points, compared with less than 5 m in the other microfacies.

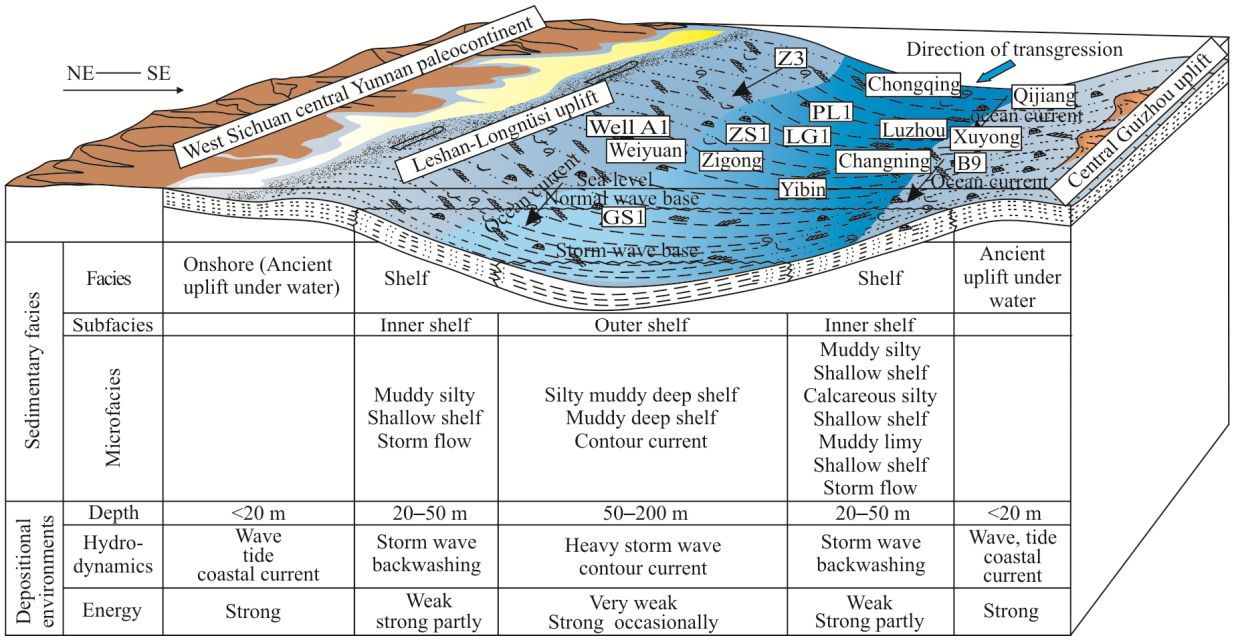

Sedimentary facies	Facies	Onshore (Ancient uplift under water)	Shelf		Shelf	Ancient uplift under water
	Subfacies		Inner shelf	Outer shelf	Inner shelf	
	Microfacies		Muddy silty Shallow shelf Storm flow	Silty muddy deep shelf Muddy deep shelf Contour current	Muddy silty Shallow shelf Calcareous silty Shallow shelf Muddy limy Shallow shelf Storm flow	
Depositional environments	Depth	<20 m	20–50 m	50–200 m	20–50 m	<20 m
	Hydro-dynamics	Wave tide coastal current	Storm wave backwashing	Heavy storm wave contour current	Storm wave backwashing	Wave, tide coastal current
	Energy	Strong	Weak strong partly	Very weak Strong occasionally	Weak Strong partly	Strong

Figure 10. Sedimentary model of Longmaxi Formation in the region of interest (viewed from *A*-*A*' direction in Fig. 9).

(c) Average *R*o is greater than 1.4 showing that the Longmaxi Formation is in mature to over-mature stages.

(d) Kerogen types are generally Type I and occasionally Type II, demonstrating good hydrocarbon potential.

(e) Clay average values of microfacies fall into a narrow range from 23.71% to 30.78%.

(f) Si average values vary greatly from 25.06% to 61.36%; Si average values of the outer shelf subfacies are greater than those of the inner shelf subfacies. The average of the muddy deep shelf microfacies reaches 61.36% and the average of muddy limy shallow shelf is the least.

(g) Average Φ values of microfacies range from 1.86% to 6.74%, falling as the calcareous component rises.

(h) *K* distribution intervals of the various microfacies are similar, average values range from 1.53×10^5 to 1.03×10^7 nD, and show no significant correlation with Φ.

(i) S_w values have a large range and no obvious distribution.

(j) *G* values of the outer shelf subfacies are generally greater than those of the inner shelf; only the *G* average value of the muddy deep shelf microfacies is over 2 m^3/t.

Comparing the measured data (Table 2) and limit values of reservoir evaluation standard (Table 1) for different sedimentary microfacies, we conclude:

The types of sedimentary microfacies influence TOC, mineral components and gas content (Fig. 8). TOC has a degree of relevance to Φ, S_w and *G*, especially when TOC is greater than 2%, indicating that the distribution of microfacies has an indirect impact on Φ and S_w (Figs. 8, 11). Therefore favorable shale gas reservoirs develop in favorable microfacies, which can be discovered through the distribution of microfacies.

TOC in the muddy deep shelf and parts of the silty muddy deep shelf microfacies are higher (average TOC>2%), and show greater hydrocarbon potential. Their thickness of intervals rich in organic materials is greater, porosity is higher, water saturation is lower and gas content is higher, demonstrating that these microfacies are advantageous for generation of hydrocarbons and accumulation of shale gas. According to the X-ray diffraction results, the siliceous materials content in these two microfacies is high, and the average value is greater than 50%; the brittleness index is high, showing that these strata are favorable to hydraulic fracturing in the production of shale gas.

The average values of TOC in other microfacies are lower, generally less than 0.5%. Although the TOC in a few horizons in the calcareous (muddy) silty shelf microfacies is relatively high, its continuous thickness is smaller for intervals with TOC>2%, which is not conducive to the accumulation and production of shale gas. The porosity in the muddy silty shallow shelf microfacies is high, a common indication of natural gas content. The lithology of the calcareous silty shallow shelf and muddy limy shallow shelf microfacies is tight, the permeability is low and water saturation is high, indicating good potential cap rocks.

The contour current and storm flow microfacies are often imbedded as lamellae in mudstone strata, and could make good reservoir strata.

From existing production test data in the region (Table 3), test production yielded greater than 0.01 MMCM/D in intervals where muddy deep shelf microfacies development is greatest, indicating that that microfacies has the strongest potential for exploration and development.

5 CONCLUSIONS

An assemblage of predominantly fine-grained continental shelf sedimentary facies is present in the Lower Silurian Longmaxi Formation in the southern region of Sichuan Basin. The continental shelf sedimentary facies can be divided into an outer shelf and an inner shelf subfacies, with the outer shelf subfacies being further divided into three microfacies: muddy deep shelf, silty muddy deep shelf and contour current microfacies; and the inner shelf subfacies being divided into four microfacies: muddy silty shallow shelf, calcareous silty

Table 2 Evaluation parameters of sedimentary microfacies (shaded data exceed the evaluation criteria shown in Table 1)

		Muddy deep shelf	Silty muddy deep shelf	Contour current	Muddy silty shallow shelf	Calcareous silty shallow shelf	Muddy limy shallow shelf	Storm flow
TOC (%)	*N*	535	861	15	179	327	60	114
	Range	0.12–9.64	0.06–8.2	0.1–1.8	0.11–9.91	0.07–642	0.1–1.82	0.1–1.82
	Average	2.35	0.83	0.52	0.66	0.78	0.34	0.29
H (m)	Range	3–41	3–36	0	1	8–16	0	0
Ro (%)	*N*	34	40	5	3	7	4	2
	Range	1.86–2.87	1.75–2.59	2.11–2.59	2.13–2.15	2.01–2.64	1.92–2.41	1.78–1.93
	Average	2.61	2.26	2.38	2.14	2.16	2.22	1.85
TI	*N*	36	33	4	2	4	10	4
	Range	64.75–92	66.5–93	57.5–77.2	88–91	72–93	68.3–84.5	47.5–85.4
	Average	81.7	83.6	63.2	89.5	85.25	76.3	56.2
Mineral components (Clay/Si, %)	*N*	221	377	15	56	211	11	72
	Range	0–73.2/17–86.3	5.6–75.9/20–92.5	20.1–40.4/29.2–73.4	6.9~38.5/23.8–77.3	0–50.4/8.8–93.4	17.6–43.1/4.9–42.3	13.1–46.4/4.9–60.2
	Average	26.19/61.36	30.78/53.38	29.11/46.4	24.37/39.28	23.71/33.93	29.71/25.06	27.44/34.35
Φ (%)/S_w (%)	*N*	130	206	10	43	75	12	3
	Range	1.95–10.27/14.56–87.31	0.7–6.11/24.30–98	0.84–12.36/30.47–86.53	0.45–6.33/23.78–89.45	0.88–6.25/20.71–83.19	0.26–4.37/27.84–76.58	0.26–7.75/25.3–73.6
	Average	4.88/39.13	2/69.08	6.74/50.72	3.43/53.27	3.03/44.26	1.86/49.29	4.12/48.23
K (nd)	*N*	74	71	6	37	46	8	2
	Range	51.5–1.87×10^7	5.55–1.84×10^7	60.7–1.93×10^7	134–1.75E7	104–6.95×10^6	4.73–5.83×10^6	180–2.06×10^7
	Average	9.47×10^6	1.47×10^6	1.53×10^5	7.8×10^6	6.4×10^5	3.4×10^5	1.03×10^7
G (m^3/t)	*N*	2	21	2	3	4	3	2
	Range	1.98–2.09	0.29–5.01	0.35–1.53	0.45–1.48	0.24–1.34	0.48–0.74	0.48–1.43
	Average	2.03	1.87	0.94	1.01	0.84	0.62	0.95

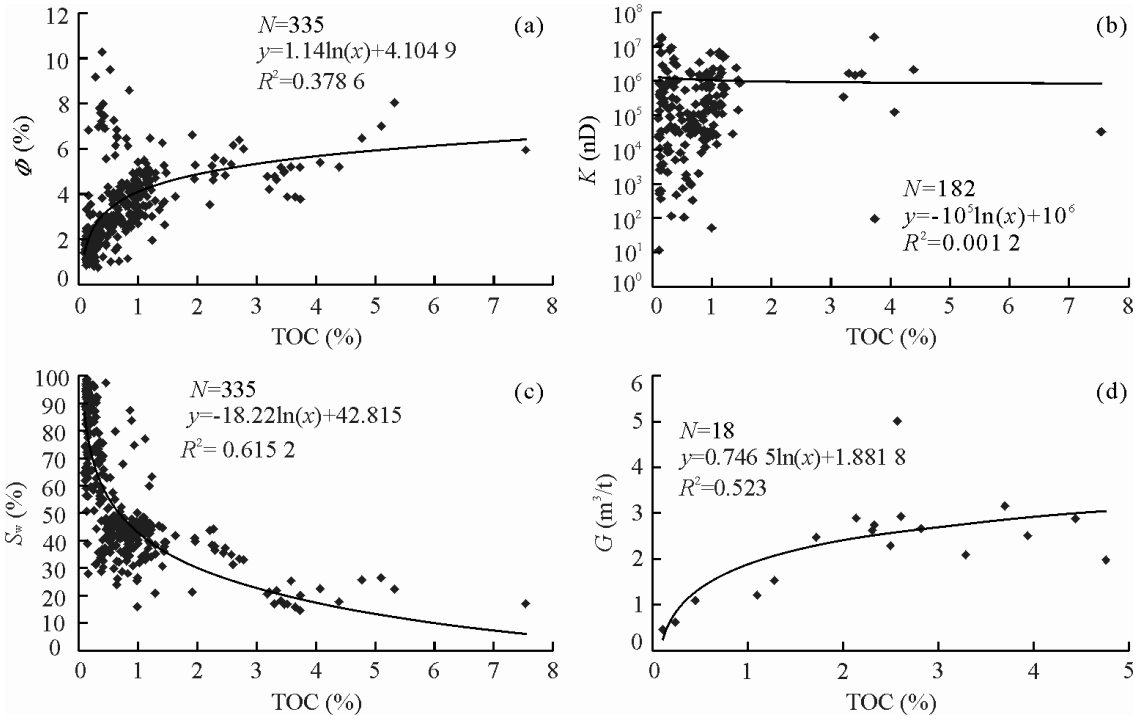

Figure 11. Scatter diagrams. (a) TOC & Φ; (b) TOC & *K*; (c) TOC & S_w; (d) TOC & *G*.

shallow shelf, muddy limy shallow shelf and storm flow microfacies. During the deposition of the Early Silurian Longmaxi Formation, the region of interest underwent two lower class (Class 4) cycles of sea level change. Each Class 4 cycle change began with a rapid marine transgression and ended with a slow marine regression. In each cycle, the content of argillaceous substances decreased from bottom to top of the strata, while content of silty or calcareous substances in the south of the region increased, giving rise to a deep water sedimentary assemblage between the Leshan-Longnüsi uplift and central Guizhou uplift trending a northwest-southeast on a continent shelf, with the thickness of sedimentary strata

Table 3 Test data of wells in the region of interest

Well	Microfacies	Depth (m)	Test yield (MMCM /D)
A1	Silty muddy deep shelf	1 511–1 535	0.002 6
A2	Muddy deep shelf	2 554–2 573	0.025
A3	Silty muddy deep shelf	3 137–3 161	0.003 9
B1	Calcareous silty shallow shelf	2 424–2 436	0.007 2
B1	Muddy deep shelf	2 495–2 516	0.01
B3	Muddy deep shelf	2 379–2 391	0.012 9
B8	Muddy deep shelf	1 299–1 319	Trace
B9	Calcareous silty shallow shelf-muddy deep shelf	3 059–3 170	0.012 6
B10	Muddy deep shelf	2 218–2 235	0.009 9

generally reducing from shelf to uplift. Nine geological evaluation parameters have been adopted: (a) TOC, total organic carbon content, (b) *H*, effective shale continuous thickness, (c) kerogen type, (d) *R*o, vitrinite reflectance, (e) mineral components, (f) *Φ*, porosity, g) *K*, permeability, h) S_w, water saturation, and (i) *G*, gas content. In evaluating microfacies for hydrocarbon potential: (a) TOC is set at a lower acceptable limit of 2%; (b) effective shale continuous thickness at a lower limit 30 m; (c) kerogen type as Type I or II; d) vitrinite reflectance lower limit 1.4%; (e) mineral composition minimum siliceous component content 40%, and clay content maximum 30%; (f) porosity lower limit 3%; (g) permeability lower limit 100 nD; (h) water saturation upper limit 40%, and (i) gas content lower limit 2 m^3/t. From measured and calculated values of these parameters, it is concluded that the muddy deep shelf and part of the silty muddy deep shelf microfacies are most favorable for the exploration of shale gas.

ACKNOWLEDGMENTS

This research was supported by the National Science and Technology Major Projects of China (No. 2012ZX05018-006-006) and the National Natural Science Foundation of China (No. U1262209). The author would also like to extend grateful thanks to PetroChina Southwest Oil and Gasfield Company for their valuable support. The final publication is available at Springer via http://dx.doi.org/ 10.1007/ s12583-015-0592-1.

REFERENCES CITED

Abouelresh, M. O., Slatt, R. M., 2012. Lithofacies and Sequence Stratigraphy of the Barnett Shale in East-Central Fort Worth Basin, Texas. *AAPG Bulletin*, 96(1): 1–22. doi:10.1306/04261110116

Aplin, A. C., Macquaker, J. H. S., 2011. Mudstone Diversity: Origin and Implications for Source, Seal, and Reservoir Properties in Petroleum Systems. *AAPG Bulletin*, 95(12): 2031–2059. doi:10.1306/03281110162

Bjørlykke, K., 2014. Relationships between Depositional Environments, Burial History and Rock Properties, Some Principal Aspects of Diagenetic Process in Sedimentary Basins. *Sedimentary Geology*, 301: 1–14. doi:10.1016/j.sedgeo.2013.12.002

Bowker, K. A., 2003. Recent Development of the Barnett Shale Play, FortWorth Basin, West Texas. *Geological Society Bulletin*, 42(6): 4–11

Bowker, K. A., 2007. Barnett Shale Gas Production, Fort Worth Basin: Issues and Discussion. *AAPG Bulletin*, 91(4): 523–533. doi:10.1306/06190606018

Boyer, C. M., Kieschinick, J., Suarez-Rivera, R., et al., 2006. Producing Gas from Its Source. Schlumberger Limited Corporation, Oilfield Review, Autumn. 37–49

Bureau of Geology and Mineral Resources of Sichuan Province, 1991. Regional Geology of Sichuan Province. Geology Press, Beijing (in Chinese)

Bureau of Geology and Mineral Resources of Sichuan Province, 1997. Multiple Classification and Correlation of the Stratigraphy of China (51)—Stratigraphy (Lithostratic) of Sichuan Province. China Uninversity of Geoscineces Press, Wuhan (in Chinese)

Chen, X., Rong, J., Li, Y., et al., 2004. Facies Patterns and Geography of the Yangtze Region, South China, through the Ordovician and Silurian Transition. *Palaeogeography*, *Palaeoclimatology*, *Palaeoecology*, 204: 353–372. doi:10.1016/S0031–0182(03)00736-3

Cluff, R. M., Dickerson, D. R., 1982. Natural Gas Potential of the New Albany Shale Group (Devonian–Mississippian) in Southeastern Illinois. SPE/DOE Symposium on Unconventional Gas Recovery, May 18–21, Pittsburgh, PA, Paper SPE/DOE 8924. 21–28

Curtis, J. B., 2002. Fractured Shale-Gas System. *AAPG Bulletin*, 86(11): 1921–1938

Dai, J., Zou, C., Liao, S., et al., 2014. Geochemistry of the Extremely High Thermal Maturity Longmaxi Shale Gas, Southern Sichuan Basin. *Organic Geochemistry*, 74: 3–12. doi:10.1016/j.orggeochem.2014.01.018

Editorial Board of Shale Gas Geology, Exploration and Development Practice Collection, 2011. Progress of Shale Gas Exploration and Development in China. Petroleum Industry Press, Beijing (in Chinese)

Fang, J., Chen, Q., Melchin, M. J., et al., 2013. Quantitative Stratigraphy of the Wufeng and Lungmachi Black Shales and Graptolite Evolution during and after the Late Ordovician Mass Extinction. *Palaeogeography*, *Palaeoclimatology*, *Palaeoecology*, 389: 96–114. doi: 10.1016/j.orggeochem.2014.01.018

Feng, G., Chen, S., 1988. Relationship between the Reflectance of Bitumen and Vitrinite in Rock. *Gas Industry*, 8(3): 20–26 (in Chinese with English Abstract)

Friedman, G. M., Sanders, J. E., 1978. Principles of Sedimentology. John Wiley and Sons, New York

Gareth, R. L., Marc, B. R., 2008. Lower Cretaceous Gas Shales

in Northeastern British Columbia, Part I: Geological Controls on Methane Sorption Capacity. *Bulletin of Canadian Petroleum Geology*, 56(1): 1–21

Gentzis, T., Goodarzi, F., 1990. A Review of the Use of Bitumen Reflectance in Hydrocarbon Exploration with Examples from Melville Island, Arctic Canada. *Rocky Mountain Section* (*SEPM*): 23–26

Guo, L., Jiang, Z., Jiang, W., 2011. Formation Condition of Gas-Bearing Shale Reservoir and Its Geological Research Target. *Geological Bulletin of China*, 30(2–3): 385–392 (in Chinese with English Abstract)

Guo, Y., Li, Z., Li, D., et al., 2004. Lithofacies Palaeogeography of the Early Silurian in Sichuan Area. *Journal of Palaeogeography*, 6(1): 20–29 (in Chinese with English Abstract)

Harris, L. D., DeWitt, W., Colton, G. W., 1978. What Are Possible Stratigraphic Controls for Gas Fields in Eastern Black Shale? *Oil and Gas Journal*, 76(14): 162–165

Hickey, J. J., Henk, B., 2007. Lithofacies Summary of the Mississippian Barnett Shale, Mitchell 2 T.P. Sims well, Wise County, Texas. *AAPG Bulletin*, 91(4): 437–443. doi:10.1306/12040606053

Hill, D. G., Lombardi, T. E., Martin, J. P., 2004. Fractured Shale Gas Potential in New York. *Northeastern Geology and Environmental Sciences*, 26(1/2): 57–78

Jarvie, D. M., Hill, R. J., Porllstro, R. M., et al., 2004. Evaluation of Hydrocarbon Generation and Storage in the Barnett Shale, Fort Worth Basin, Texas. Ellison Miles Memorial Symposium, Farmers Branch, Texas. 22–23

Jarvie, D. M., Hill, R. J., Ruble, T. E., et al., 2007. Unconventional Shale Gas Systems: the Mississippian Barnett Shale of North Central Texas as One Model for Thermogenic Shale Gas Assessment. *AAPG Bulletin*, 91(4): 475–499. doi:10.1306/12190606068

Jenkins, C. D., Boyer, C. M., 2008. Coalbed- and Shale-Gas Reservoirs. *JPT*, 60(1): 92–99

Jia, C., Zheng M., Zhang Y., 2012. Unconventional Hydrocarbon Resources in China and the Prospect of Exploration and Development. *Petroleum Exploration and Development*, 39(2): 139–146. doi:10.1016/S1876-3804(12)60026–3

Li, T., 1991. The Principal Geological Feature of Oil-Forming Formation in Sichuan Basin. *Mineralogy and Petrology*, 11(3): 80–87 (in Chinese with English Abstract)

Li, Y., Fan, T., Gao, Z., et al., 2012. Sequence Stratigraphy of Silurian Black Shale and Its Distribution in the Southeast Area of Chongqing. *Natural Gas Geoscience*, 23(2): 299–306 (in Chinese with English Abstract)

Liang, C., Jiang, Z., Yang, Y., et al., 2012. Characteristics of Shale lithofacies and Reservoir Space of the Wufeng-Longmaxi Formation, Sichuan Basin. *Petroleum Exploration and Development*, 39(6): 691–698. doi: 10.1016/S1876–3804(12)60098-6

Liang, D., Guo, T., Bian, L., et al., 2008. Some Progresses on Studies of Hydrocarbon Generation and Accumulation in Marine Sedimentary Regions, Southern China (Part 1): Distribution of Four Suits of Regional Marine Source Rocks. *Marine Oil and Gas Geology*, 13(2): 1–16 (in Chinese with English Abstract)

Liang, D., Guo, T., Bian, L., et al., 2009. Some Progresses on Studies of Hydrocarbon Generation and Accumulation in Marine Sedimentary Regions, Southern China (Part 3): Controlling Factors on the Sedimentary Facies and Development of Palaeozoic Marine Source Rocks. *Marine Oil and Gas Geology*, 14(2): 1–19 (in Chinese with English Abstract)

Lin, B., Su, Y., Zhu, X., et al., 1998. Stratigraphy of China (Silurian). Geology Press, Beijing (in Chinese)

Liu, B., Xu, X., 1994. Atlas of the Lithofacies and Palaeogeography of South China (Sinian–Triassic) (English Edition). Science Press. Beijing

Liu, S., Deng, B., Li, Z., et al., 2012. Architecture of Basin-Mountain Systems and Their Influences on Gas Distribution: A Case Study from the Sichuan Basin, South China. *Journal of Asian Earth Sciences*, 47: 204–215. doi:10.1016/j.jseaes.2011.10.012

Loucks, R. G., Ruppel, S. C., 2007. Mississippian Barnett Shale: Lithofacies and Depositional Setting of a Deep-Water Shale-Gas Succession in the Fort Worth Basin, Texas. *AAPG Bulletin*, 91(4): 579–601. doi:10.1306/11020606059

Loydell, D. K., 1998. Early Silurian Sea-Level Changes. *Geological Magazine*, 135(4): 447–471

Ma, L., Chen, H., Gan, K., et al., 2004. Tectonics and Marine Oil and Gas Geology in South China. Geology Press, Beijing (in Chinese)

Ma, Y., Chen, H., Wang, G., et al., 2009. Sequence Stratigraphy and Palaeogeography of South China. Science Press. Beijing (in Chinese)

Martineau, D. F., 2007. History of the Newark East Field and the Barnett Shale as a Gas Reservoir. *AAPG Bulletin*, 91(4): 399–403. doi:10.1306/intro910407

Meyers, P. A., 2006. Paleoceanographic and Paleoclimatic Similarities between Mediterranean Sapropels and Cretaceous Black Shales. *Palaeogeography*, *Palaeoclimatology*, *Palaeoecology*, 235: 305–320. doi:10.1016/j.palaeo.2005.10.025

Montgomery, S. L., Jarvie, D. M., Bowker, K. A., et al., 2005. Mississippian Barnett Shale, Fort Worth Basin, North-Central Texas: Gas Shale Play with Multi-Trillion Cubic Foot Potential. *AAPG Bulletin*, 89: 155–175. doi:10.1306/09170404042

Mu, C., Zhou, K., Liang, W., et al., 2011. Early Paleozoic Sedimentary Environment of Hydrocarbon Source Rocks in the Middle–Upper Yangtze Region and Petroleum and Gas Exploration. *Acta Geologica Sinica*, 85(4): 526−532 (in Chinese with English Abstract)

Mu, E., Zhu, Z., Chen, J., et al., 1983. Silurian in Shuanghe Changning, Sichuan. *Journal of Stratigraphy*, 7(3): 208–215 (in Chinese)

Mu, E., Boucot, A. J., Chen, X., et al., 1986. Correlation of the Silurian Rocks of China. *Special Paper of the Geological Society of America*, 202: 1–80. doi:10.1130/SPE202–p1

Picard, M. D., 1971. Classification of Fine-Grained Sedimentary Rocks. *Journal of Sedimentary Research*, 41(1): 179–195

Pollastro, R. M., 2003. Geological and Production

Characteristics Utilized in Assessing the Barnett Shale Continuous (Unconventional) Gas Accumulation. In: Barnett–Paleozoic Total Petroleum System, Fort Worth Basin, Texas: Barnett Shale Symposium. Ellison Miles Geotechnology Institute at Brookhaven College, November 12–13, Dallas, Texas. 6

Potter, P. E., Maynard, J. B., Depetris, P. J., 2005. Mud and Mudstones. Springer-Verlag, Berlin Heidelberg

Slatt, R. M., Philp, P. R., Abousleiman, Y., et al., 2012. Pore-to-Regional-Scale Integrated Characterization Workflow for Unconventional Gas Shales. In: Breyer, J. A., ed., Shale Reservoirs—Giant Resources for the 21st Century. *AAPG Memoir*, 97: 127–150

Slatt, R. M., Rodriguez, N. D., 2012. Comparative Sequence Stratigraphy and Organic Geochemistry of Gas Shales: Commonality or Coincidence? *Journal of Natural Gas Science and Engineering*, 8: 68–84. doi:10.1016/j.jngse.2012.01.008

Sondergeld, C. H., Newsham, K. E., Comisky, J. T., et al., 2010. Petrophysical Considerations in Evaluating and Producing Shale Gas Resources. SPE Unconventional Gas Conference, February, 23–25, Pittsburgh, Pennsylvania, USA.

Stevenson, D. L., Dickerson, D. R., 1969. Organic Geochemistry of the New Albany Shale in Illinois. *Illinois State Geological Survey*, *Illinois Petroleum*, 90: 1–11

Committee of Petroleum Geology Exploration of Professional Standards, 2012. Determination of Vitrinite Reflectance in Sedimentary Rocks: SY/T 5124–2012. Standards Press of China, Beijing

Committee of Petroleum Geology Exploration of Professional Standards, 1996. Indentification of Maceral and Division of Kerogen Type by Transmitted and Fluorescent Light: SY/T 5125-1996. Standards Press of China, Beijing

Committee of Petroleum Geology Exploration of Professional Standards, 2010. Analysis Method for Clay Minerals and Ordinary Non-Clay Minerals in Sedimentary Rocks by X–ray Diffraction: SY/T 5163-2010. Standards Press of China, Beijing

Committee of Petroleum Geology Exploration of Professional Standards, 2013. Measurement Method of Shale Gas Content: SY/T 6940-2013. Standards Press of China, Beijing

Committee of Petroleum Geology Exploration of Professional Standards, 2003. Determination of Total Organic Carbon in Sedimentary Rock: GB/T 19145-2003. Standards Press of China, Beijing

Wang, H., 1985. Atlas of the Palaeogeography of China. China Cartographic Press, Beijng (in Chinese)

Whelan, J. K., Thompson-Rizer, C. L., 1993. Chemical Methods for Assessing Kerogen and Protokerogen Types and Maturity. In: Michael, H. E., Stephen, A. M., eds., Organic Geochemistry. Plenum Press, New York. 289–353

Wignall, P. B., 1991. Model for Transgressive Black Shales? *Geology*, 19(2): 167–170

Xiao, X., Liu, D., Fu, J., 1991. The Significance of Bitumen Reflectance as a Mature Parameter of Source Rocks. *Acta Sedimentologica Sinica*, 9 (Suppl.): 138–146 (in Chinese with English Abstract)

Zhai, G. M., Wang, S. S., 1989. Petroleum Geology of China, Part 10: Sichuan Petroleum Region. Petroleum Industry Press, Beijing (in Chinese)

Zheng, H., Hu, Z., 2010. Atlas of Tectonic and Lithofacies Palaeogeography in Pre-Mesozoic in China. Geology Press, Beijing. 1–194

Zheng, H., Gao, B., Peng, Y., et al., 2013. Sedimentary Evolution and Shale Gas Exploration Direction of the Lower Silurian in Middle–Upper Yangtze Area. *Journal of Palaeogeography*, 15(5): 645–656. doi:10.7605/gdlxb. 2013.05.052 (in Chinese with English Abstract)

Zhou, M., Wang, R., Li, Z., et al., 1993. Ordovician and Silurian Lithofacies Palaeogeography and Mineralization in South China. Geology Press, Beijng (in Chinese)

Zou, C., Dong, D., Wang, S., et al., 2010. Geological Characteristics and Resource Potential of Shale Gas in China. *Petroleum Exploration and Development*, 37(6): 641–653. doi:10.1016/S1876–3804(11)60001–3

Zou, C., Tao, S., Hou, L., et al., 2013. Unconventional Petroleum Geology (2nd Ed.). Geology Press, Beijing. 127–129 (in Chinese)